Biophysical Reports

ARTICLE

Molecular understanding of calorimetric protein unfolding experiments

Joachim Seelig[1,*] and Anna Seelig[1]
[1]Biozentrum, University of Basel, Basel, Switzerland

ABSTRACT Testing and predicting protein stability gained importance because proteins, including antibodies, became pharmacologically relevant in viral and cancer therapies. Isothermal scanning calorimetry is the principle method to study protein stability. Here, we use the excellent experimental heat capacity $C_p(T)$ data from the literature for a critical inspection of protein unfolding as well as for the test of a new cooperative model. In the relevant literature, experimental temperature profiles of enthalpy, $H_{cal}(T)$, entropy, $S_{cal}(T)$, and free energy, $G_{cal}(T)$ are missing. First, we therefore calculate the experimental $H_{cal}(T)$, $S_{cal}(T)$, and $G_{cal}(T)$ from published $C_p(T)$ thermograms. Considering only the unfolding transition proper, the heat capacity and all thermodynamic functions are zero in the region of the native protein. In particular, the free energy of the folded proteins is also zero and $G_{cal}(T)$ displays a trapezoidal temperature profile when cold denaturation is included. Second, we simulate the DSC-measured thermodynamic properties with a new molecular model based on statistical-mechanical thermodynamics. The model quantifies the protein cooperativity and predicts the aggregate thermodynamic variables of the system with molecular parameters only. The new model provides a perfect simulation of all thermodynamic properties, including the observed trapezoidal $G_{cal}(T)$ temperature profile. Importantly, the new cooperative model can be applied to a broad range of protein sizes, including antibodies. It predicts not only heat and cold denaturation but also provides estimates of the unfolding kinetics and allows a comparison with molecular dynamics calculations and quasielastic neutron scattering experiments.

WHY IT MATTERS Protein stability is an important issue in the development of pharmaceutical biologics. Because biologics are often large molecules (e.g., antibodies), and as folding is a highly cooperative process, a new model is proposed that takes into account cooperativity and protein size. The model is based on a consistent set of thermodynamic parameters, derived from differential scanning calorimetry (DSC) experiments. Here, we apply the model to published DSC data of four very different proteins to demonstrate its predictive power. It not only yields heat denaturation but also cold denaturation, as well as the kinetics of unfolding. Moreover, the results of the cooperative model can be compared with molecular dynamics calculations.

INTRODUCTION

Protein stability is a *most relevant* issue in the development of pharmaceutical biologics. Thermodynamic aspects of protein *un*folding have acquired significant practical importance because they provide the theoretical framework for rational protein design and protein modifications (1). Differential scanning calorimetry (DSC) is the method of choice for thermodynamic studies of protein folding/unfolding equilibria (2,3). Analysis of DSC experiments with simple thermodynamic models has been key for developing our understanding of protein stability (4). So far, the reversible denaturation reaction has been analyzed with a two-state model (5).

However, the protein folding ⇄ unfolding equilibrium is a dynamic reaction with many short-lived intermediates (6). A multistate cooperative algorithm is therefore a physically more realistic alternative. We have shown for several proteins that the cooperative multistate Zimm-Bragg theory is such an alternative (7–14). The theory yields a quantitated measure of cooperativity, is not limited in protein size, and provides excellent simulations of protein unfolding thermodynamics. Here, we present a significant improvement of the model by combining the Zimm-Bragg theory with statistical mechanics. As a result, the macroscopic thermodynamic properties of heat unfolding and cold denaturation can

Submitted September 9, 2021, and accepted for publication December 2, 2021.

*Correspondence: joachim.seelig@unibas.ch

Editor: Jörg Enderlein.

https://doi.org/10.1016/j.bpr.2021.100037

be explained with molecular parameters of well-defined physical meaning. The new model is validated by analyzing published DSC measurements of lysozyme (10), the classic example of protein unfolding, gpW62 (15), an ultrafast folding protein, mAb, a large monoclonal antibody (13), metmyoglobin (16), a protein exhibiting cold denaturation, and ubiquitin, an α-helical protein (17). In the long-standing history of DSC of protein unfolding, the heat capacity function $C_p(T)$ was mainly used to evaluate the enthalpy change ΔH_{cal} of the unfolding transition. Entropy and free energy were ignored, although both properties are easily derived from $C_p(T)$. Here, we systematically evaluate the complete temperature profiles $H_{cal}(T)$, $S_{cal}(T)$, and $G_{cal}(T)$ from experimental $C_p(T)$ data and analyze them with the cooperative multistate Zimm-Bragg theory. In particular, the free energy is found to display a trapezoidal shape with a zero free energy in the region around the native protein. This unique thermodynamic signature is precisely predicted by the Zimm-Bragg theory, but disagrees with the parabolic shape predicted by the two-state model. The Zimm-Bragg analysis covers DSC experiments in the temperature range of 20–90°C. The same fit parameters can be used to calculate the entropies of completely denatured proteins at a denaturation temperature of 225°C. Excellent agreement with the predictions of the Dynameomics Entropy Dictionary is obtained (18).

MATERIALS AND METHODS

This study describes a new model for protein unfolding, which is based on the multistate, cooperative Zimm-Bragg theory. The most significant accomplishment of this model is that it enables us to calculate the aggregate thermodynamic variables from molecular parameters. The total energy, entropy, and free energy are derived in terms of a continuous canonical partition function or its derivatives. It is an analytical model expressing the macroscopic thermodynamic properties of the system with molecular parameters only.

The potential of the model is illustrated with published DSC experiments of protein unfolding. In DSC the heat capacity $C_p(T) = (\partial H/\partial T)p$ is recorded as a function of temperature. In protein unfolding, $C_p(T)$ is composed essentially of two parts, the basic heat capacity of the native protein and that of the phase transition proper. Native lysozyme, for example, has a basic heat capacity of ~5 kcal/molK, which increases to ~25 kcal/molK at the midpoint of unfolding, and decreases again to ~7.2 kcal/molK for the unfolded protein (19,20). The basic heat capacity makes a large contribution to the thermodynamic properties and dominates enthalpy, entropy, and free energy (cf. Fig. 2). Therefore, it is common practice to apply a baseline correction such that the heat capacity of the native protein is zero (4,21). As a consequence of this subtraction it follows that all thermodynamic properties are zero in the region of the native protein, including the free energy. The model was tested with published DSC data of proteins ranging in size between 62 and 1200 amino acid (aa) residues. In three examples the published data were already baseline corrected. In one example we present both raw and baseline-corrected data.

The $C_p(T)$ thermograms were integrated (Eqs. 10, 11, and 12), yielding the temperature profiles $H_{cal}(T)$, $S_{cal}(T)$, and $G_{cal}(T)$ of the unfolding transition. Such experimental profiles are missing in the relevant literature. Here, they are evaluated from experimental data for all four proteins investigated.

The theoretical analysis proceeds as follows. The heat capacity $C_p(T)$ is simulated with the cooperative model presented below. The fit parameters are rather independent of each other and are determined sequentially. The unfolding enthalpy h_0 per amino acid residue is ~1.1 ± 0.2 kcal/mol (10). The number of amino acid residues in the unfolding reaction is $\nu \sim \Delta H_{cal}/h_0$. Here, ΔH_{cal} is the total heat of unfolding. The cooperativity parameter σ is typically $\sigma \sim 10^{-3} - 10^{-7}$. σ is easily adjusted by fitting the sharp transition peak. Finally, the heat capacity c_v is determined by fitting the observed increase in heat capacity ΔC_p^0. No global fit procedure is needed as all four parameters can be determined precisely by a judicial inspection of the experimental data. The same parameters are then used to calculate enthalpy $H_{cal}(T)$, entropy $S_{cal}(T)$, and free energy $G_{cal}(T)$.

The popular two-state model is briefly discussed as far as the free energy is concerned. The model is restricted to the unfolding transition proper and is applied to baseline-corrected thermograms. It assumes a zero heat capacity for the native protein (3,22,23). However, in disagreement with DSC, the model predicts a positive free energy for the region of the native protein. An alternative two-state model with correct thermodynamic predictions has been published (24).

All calculations presented in this study were performed with MathCad 15. In this program, all equations can be written as shown in the text.

Theory

Zimm-Bragg theory extended to cold denaturation

Protein unfolding is a dynamic process in which individual amino acid residues flip from their native (n) to their unfolded (u) state. Rapid equilibria between many short-lived intermediates can be expected. An early example of cooperative unfolding is the α-helix to random coil transition of synthetic peptides described with the Zimm-Bragg theory (25–27). The cooperative folding theory distinguishes between a growth process with an equilibrium constant q(T) and a nucleation step with an equilibrium constant $\sigma q(T)$, where σ is the cooperativity or nucleation parameter. Growth is defined as the addition of a new helical segment to an already existing α-helix. Nucleation is the formation of a new helical segment within an unstructured region. The steepness of the transition is determined by the cooperativity parameter σ.

The central element of the *original* Zimm-Bragg theory is a discrete canonical partition function of the form $Z(T) = \sum e^{\frac{-E_i}{RT}}$, which collects all the energetic states of the folding process. The system is allowed to exchange heat with its environment, but its volume and the number of particles are fixed. The volume changes in protein unfolding are indeed very small (28,29) and can be neglected in the present analysis. The rather lengthy expressions of the partition function Z(T) in the initial Zimm-Bragg theory (25) can be written in compact form (27).

$$Z(T) = \begin{pmatrix} 1 & 0 \end{pmatrix} \begin{pmatrix} 1 & \sigma q(T) \\ 1 & q(T) \end{pmatrix}^{\nu} \begin{pmatrix} 1 \\ 1 \end{pmatrix}. \qquad (1)$$

ν denotes the number of amino acid residues involved in unfolding. The cooperativity parameter is small with $\sigma \sim 10^{-3}$–10^{-7}. The larger σ, the less cooperative is the system and the broader is the transition peak. The limit of no cooperativity is reached with $\sigma = 1$. At this condition the Zimm-Bragg theory reduces to a two-state model, similar to the chemical two-state model, but providing a more stringent thermodynamic interpretation of DSC thermograms. The chain length ν also has some influence on the width of the transition. The smaller ν, the

broader is the unfolding transition. Short chains lead a broad transition (26).

The equilibrium constant q(T) is given by

$$q(T) = e^{\frac{-h(T)}{R}\left(\frac{1}{T}-\frac{1}{T_\infty}\right)}. \quad (2)$$

h(T) is the enthalpy needed to induce the n → u conformational change. Up until now, this parameter was assumed to be temperature-independent with $h_0 \sim 0.9$–1.3 kcal/mol (26,30–33). Here, we introduce a temperature-dependent unfolding enthalpy, which changes Eq. 1 to a continuous canonical partition function

$$h(T) = h_0 + c_v(T - T_0). \quad (3)$$

T_0 is the midpoint temperature of heat-induced unfolding. The heat capacity c_v refers to the unfolding of a single amino acid residue. The reference temperature T_∞ in Eq. 2 determines the position of the heat capacity maximum on the temperature axis. It is identical with T_0 if the number of amino acid residues ν is much larger than $\sigma^{-1/2}$.

The fraction of unfolded protein $\Theta_U(T)$ is

$$\Theta_U\left(T\right) = \frac{q(T)}{\nu}\frac{d(\ln Z(T))}{dT}\left(\frac{dq(T)}{dT}\right)^{-1}. \quad (4)$$

For a noncooperative system with $\sigma = 1$ the multistate Zimm-Bragg theory reduces to a two-state model as mentioned above (14).

Cold denaturation

The heat capacity term c_v has two consequences. First, c_v produces the heat capacity increase ΔC_p^0 of the unfolded protein. Second, c_v leads to an additional transition at low temperature (cold denaturation). The exponent in the equilibrium constant q(T) (Eq. 2) has zeros at T_0 and at $h(T) = 0$. The latter relation leads to

$$T_c = T_0 - \frac{h_0}{c_v}. \quad (5)$$

T_0 is the midpoint of heat denaturation, T_c that of cold denaturation. The temperature difference between heat and cold denaturation is $\Delta T = h_0/c_v$.

Partition function and statistical-mechanical thermodynamics

We show that the thermodynamics of protein unfolding and, consequently, the DSC experiments can be simulated without macroscopic fit parameters. According to statistical-mechanical thermodynamics, the partition function Z(T) is the sum of all conformational energies and is sufficient to determine the thermodynamic system parameters, that is, the inner energy E(T), the entropy S(T), and the Helmholtz free energy F(T) (34,35). The relevant equations are as follows

$$F(T) = -RT\ln Z(T), \quad (6)$$

$$E(T) = RT^2\frac{d\ln Z(T)}{dT} + \int_{T_{ini}}^{T} C_p(T)dT, \quad (7)$$

$$S(T) = \frac{E(T) - F(T)}{T} + \int_{T_{ini}}^{T}\frac{C_p(T)}{T}dT, \quad (8)$$

$$C_V(T) = \frac{dE(T)}{dT} + C_p(T). \quad (9)$$

The first term on the right side determines the phase transition proper. The second terms is the contribution of the basic protein heat capacity $C_p(T)$, which is independent of the unfolding transition. The experimental data can thus be analyzed without any arbitrary baseline correction. In baseline-corrected thermograms the heat capacity of the native protein is $C_p(T) = 0$ kcal/molK and only the first terms need to be considered. For $C_p(T) \neq 0$ kcal/molK Eq. 6 must be replaced by $F(T) = E(T) - TS(T)$, where E(T) and S(T) are given by Eqs. 7 and 8, respectively. Integration starts at T_{ini}, the temperature at the beginning of the DSC measurement. In almost all published examples, a baseline correction is performed and a zero heat capacity is assigned to the native protein. This is necessary as neither the chemical two-state model nor the Zimm-Bragg theory account for the basic protein heat capacity. The inclusion of a $C_p(T)$ term obscures the phase transition proper. This is illustrated in Fig. 2, where the original DSC data are compared with the baseline-corrected results.

DSC

DSC is the method of choice to determine the thermodynamic properties of protein unfolding. DSC measures the temperature course of the heat capacity $C_p(T)$, which includes not only the conformational enthalpy proper but also the increase in heat capacity ΔC_p^0 between native and denatured protein (36,37). Stepwise integration of $C_p(T)$ provides unfolding enthalpy, entropy, and Gibbs free energy:

$$H(T_i) = \sum_1^i\left[\frac{C_p(T_i) + C_p(T_{i+1})}{2}\right][T_{i+1} - T_i], \quad (10)$$

$$S(T_i) = \sum_1^i\frac{C_p(T_{i+1}) + C_p(T_i)}{2T_i}[T_{i+1} - T_i], \quad (11)$$

$$G(T_i) = H(T_i) - T_iS(T_i). \quad (12)$$

"It is clear that in considering the energetic characteristics of protein unfolding one has to take into account all energy which is accumulated upon heating and not only the very substantial heat effect associated with gross conformational transitions, that is, all the excess heat effects must be integrated" (23). The DSC-measured thermodynamic parameters characterizing the total unfolding transition are denoted ΔH_{cal}, ΔS_{cal}, and ΔG_{cal}.

DSC measurements are made at constant pressure. As mentioned above, the volume changes in protein unfolding are very small (<5%) and the following relations are valid without loss of accuracy. Heat capacity $C_p(T) \cong C_v(T)$, enthalpy $H(T) \cong$ inner energy E(T), entropy $S_p(T) \cong S_v(T)$, Gibbs free energy $G(T) \cong$ Helmholtz free energy F(T).

RESULTS

Our earlier simulations of DSC experiments with the Zimm-Bragg theory required molecular as well as macroscopic fit parameters. The extent of unfolding $\Theta_U(T)$ was calculated with molecular parameters (h_0, σ) and was then multiplied with macroscopic parameters, that is, the unfolding enthalpy ΔH_0 and the

heat capacity increase ΔC_p^0. Here, we eliminate ΔH_0 and ΔC_p^0 by combining the partition function Z(T) with statistical-mechanical thermodynamics (Eqs. 6, 7, 8, and 9). All macroscopic thermodynamic properties are now predicted exclusively with molecular parameters (h_0, c_v, σ, ν). Of particular interest is the free energy of unfolding $G(T) \cong F(T)$. Proposed as a parabolic function in the theory of the two-state model, the DSC-accessible free energy $G_{cal}(T)$ (Eq. 12) appears to be completely ignored in *the relevant DSC literature*. In the following we compare proteins of different size and structure, which were carefully studied with DSC. The analysis of the $C_p(T)$ thermograms provides the caloric, model-independent results for enthalpy $H_{cal}(T)$, entropy $S_{cal}(T)$, and free energy $G_{cal}(T)$. The measured thermodynamic properties are then compared with the predictions by the cooperative Zimm-Bragg theory and the two-state model.

Lysozyme unfolding: DSC and molecular multistate partition function

Lysozyme is a 129-residue protein composed of ~25% α-helix, ~40% β-structure, and ~35% random coil in solution at room temperature (10). Upon unfolding, the α-helix is almost completely lost and the random coil content increases to ~60%. Thermal unfolding is completely reversible and lysozyme is the classical example to demonstrate two-state unfolding (2,20,22). Fig. 1 *A* shows the $C_p(T)$ thermograms of lysozyme unfolding with a resolution of 0.17°C (10) Unfolding takes place in the temperature range of $45°C \leq T \leq 73°C$ (midpoint temperature $T_0 = 61.7°C$). The unfolding enthalpy is $\Delta H_{cal} = 147$ kcal/mol (Eq. 10) and the entropy $\Delta S_{cal} = 0.437$ kcal/molK (Eq. 11). The enthalpy/entropy ratio $\Delta H_{cal}/\Delta S_{cal} = 335.5\ K = 62.5°C$ agrees with the midpoint temperature T_0. The molar heat capacity of unfolded lysozyme increases by $\Delta C_p^0 = 2.269$ kcal/molK, in agreement with literature data (22,36,37).

The high cooperativity of lysozyme unfolding (cooperativity parameter $\sigma = 1.0 \times 10^{-6}$) leads to a sharp unfolding transition, which is well approximated by a two-state equilibrium. Two-state model and Zimm-Bragg theory both provide excellent simulations of the heat capacity $C_p(T)$ (Fig. 1 *A*).

Differences between the two models exist, however, in predicting the temperature dependence of the free energy. The two-state model defines the free energy as

$$\Delta G(T) = \Delta H_0\left(1 - \frac{T}{T_0}\right) + \Delta C_p^0(T - T_0) - T\Delta C_p^0 \ln\left(\frac{T}{T_0}\right), \quad (13)$$

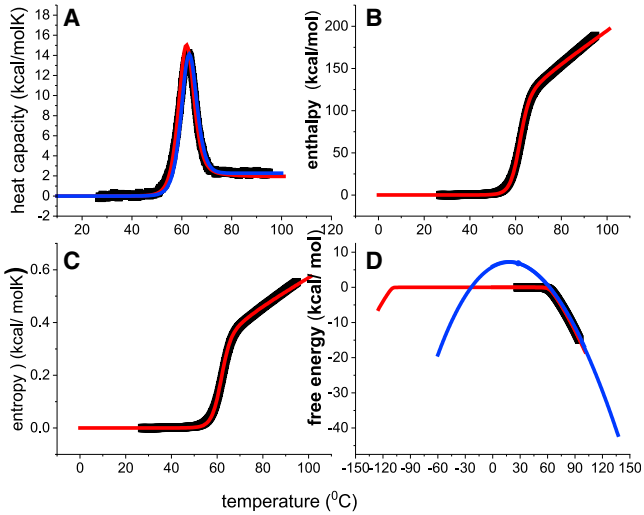

FIGURE 1 Differential scanning calorimetry of 50 μM lysozyme in 20% glycine buffer, pH 2.5. Black data points: DSC thermograms obtained with a heating rate of 1°C min^{-1} and a step size of 0.17°C. Red lines: simulations with the Zimm-Bragg theory with $h_0 = 1.0$ kcal/mol, $c_v = 6$ cal/molK, $\sigma = 1.0 \times 10^{-6}$, $\nu = 129$. (*A*) Heat capacity $C_p(T)$. (*B*) Unfolding enthalpy H(T). (*C*) Unfolding entropy S(T). (*D*) Free energy of unfolding G(T). Blue line: $\Delta G(T)$ (Eq. 13) predicted by the two-state model calculated with a conformational enthalpy $\Delta H_0 = 107$ kcal/mol and a heat capacity increase $\Delta C_p^0 = 2.269$ kcal/mol. Data taken from reference (10).

yielding the parabolic shape in Fig. 1 *D* (*blue line*, same parameters as in Fig. 1 *A*). The free energy has a positive maximum of 7.18 kcal/mol for the native protein at 20°C and becomes zero at $T_0 = 62°C$, where lysozyme is 50% unfolded. However, this is not what is seen in the DSC experiment (Fig. 1 *D*, *black data points*). The free energy of the native protein is zero and becomes immediately negative upon unfolding. Between 27°C and T_0 the DSC experiment reports a negative free energy change $\Delta G_{cal} = -0.7$ kcal/mol, which increases rapidly beyond T_0 to $\Delta G_{cal} = -6.06$ kcal/mol at 73°C (90% unfolding). The Zimm-Bragg theory (Eq. 7) reproduces precisely the DSC result (Fig. 1 *D*, *red line*). Extending this simulation to low temperatures yields cold denaturation at $T_{cold} = -103°C$. The Zimm-Bragg theory thus predicts a trapezoidal shape of the free energy and the flat, near zero region extends over almost 140°C. An experimental proof for the free energy trapezoidal shape is given in Fig. 4.

gpW62, an ultrafast folding protein

gpW62 is a 62-residue $\alpha+\beta$ protein that belongs to a group of ultrafast folding proteins (4,15). gpW62 folding was investigated with a variety of techniques, including DSC. Fig. 2 *A* shows the original heat capacity $C_p(T)$ (7) from Fig. 4 *A* of reference (15)) and the baseline-corrected $C_p(T)$ (■). Baseline correction was achieved by

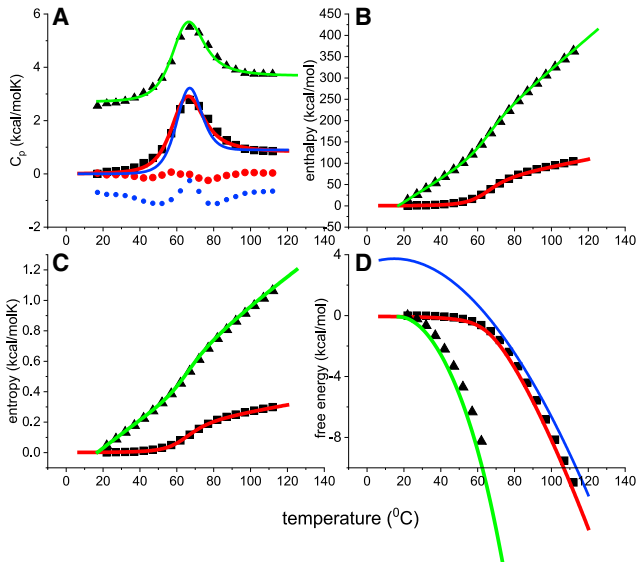

FIGURE 2 gpW62 DSC unfolding (7). (▲) Original $C_p(T)$ data (taken from Fig. 4 *A* in reference (15)). (■) Baseline-corrected data. Data points in (*B–D*) were calculated from data points in (*A*) with Eqs. 10, 11, and 12. Red lines: simulations of unfolding transition proper with the Zimm-Bragg theory ($h_0 = 1.26$ kcal/mol, $c_v = 5$ cal/molK, $\sigma = 5.0 \times 10^{-4}$, $\nu = 62$ residues). Blue lines: two-state model ($\Delta H_0 = 49$ kcal/mol, $\Delta C_p^0 = 0.9$ kcal/molK). The red dotted lines in (*A*) are the differences between the experimental DSC data and the simulations. For better visibility, the blue dotted line is shifted by −1 kcal/molK. Green lines: sum of Zimm-Bragg theory and the contribution of the basic heat capacity of the native protein $C_p = 2.7$ kcal/molK (cf. Eqs. 7, 8, and 9).

simply subtracting the heat capacity of the native protein of 2.7 kcal/molK. Both data sets were simulated with Eq. 9, either with C_p (green line) or without C_p (red line). The blue line is the best fit with the chemical two-state model (calculated with Eq. 14 of reference (3)). The dotted lines in Fig. 2 *A* are the differences between experimental results and simulations. Equations 10, 11, and 12 were applied to both the original and the baseline-corrected $C_p(T)$ data yielding experimental results for enthalpy (Fig. 2 *B*), entropy (Fig. 2 *C*), and Gibbs free energy (Fig. 2 *D*). In the uncorrected data (7) the unfolding transition is masked by the very substantial contribution of the basic heat capacity $C_p = 2.7$ kcal/molK. Still, it should be noted that the Gibbs free energy of the native protein is zero, even for the noncorrected heat capacity data. In the following we only discuss the baseline-corrected data.

The midpoint temperature is $T_0 = 67°C$. The unfolding enthalpy is $\Delta H_{cal} = 91.7$ kcal/mol, measured between 37 and 102°C. This is a large enthalpy for a 62-residue protein. The free energy change between native and unfolded gpW62 is $\Delta G_{cal} = -8.11$ kcal/mol. The free energy per amino acid residue $g_{cal} = -131$ cal/mol is almost three times larger than that of lysozyme with $g_{cal} = -47$ cal/mol.

Several aspects of the gpW62 folding equilibrium are unusual. The cooperativity is low with $\sigma = 5 \times 10^{-4}$ and unfolding extends over a broad temperature range of $\Delta T \sim 65°C$. This may be compared with lysozyme with $\sigma = 1 \times 10^{-6}$ and $\Delta T \sim 30°C$. As the transition is broad, the Zimm-Bragg theory provides a better fit than the two-state model (Fig. 2 *A*). The low cooperativity facilitates fast folding by a low nucleation free energy (see Discussion). Fast folding of gpW62 could also be promoted by the large free energy change of the unfolding reaction. According to the thermodynamics of irreversible processes, the chemical reaction rate is proportional to the affinity, i.e., the free energy, of the reaction (38–40). The ultrafast folding of gpW62 could thus arise from the combination of a low nucleation energy and a large unfolding affinity.

Monoclonal antibody mAb

The two-state model works best for enthalpies of 50–200 kcal/mol. No such limitation exists for the Zimm-Bragg theory. This is demonstrated for the recombinant monoclonal IgG1 antibody mAb (143 kDa, ∼1280 aa), the main transition of which has an enthalpy of ∼1000 kcal/mol (13). The antibody is formed of two identical heavy chains of ∼450 residues each and two identical light chains of ∼200 residues. The heavy and light chains fold into domains of ∼110 aa residues. The secondary structure of mAb is composed of 7–11% α-helix and 40–45% β-sheet (41).

The DSC experiment (Fig. 3 *A*) reveals a pretransition at 73°C and a main transition at 85°C. The unfolding enthalpy of the pretransition is $\Delta H_{cal} = 290$ kcal/mol involving $\nu_{pre} = \Delta H_{cal}/h_0 = 263$ aa residues. The main transition has an enthalpy of $\Delta H_{cal} \simeq 1000$ kcal/mol with $\nu_{main} \simeq 880$ aa residues. Taken together, pre- and main transition account for ∼90% of all amino acid residues. A molecular interpretation of pre- and main transition based on the mAb structure has been given (13). The pretransition results from the unfolding of two C_{H2} domains, whereas the main transition represents the unfolding of eight domains of the Fab fragment and two domains of the Fc fragment. In Fig. 3 the pretransition (*green*) and main transition (*violet*) are superimposed (*red*). The pretransition is slightly less cooperative with $\sigma = 5 \times 10^{-5}$ than the main transition with $\sigma = 2 \times 10^{-5}$. The same molecular parameters $h_0 = 1.1$ kcal/mol and $c_v = 7.0$ cal/molK were used in all simulations. The theory predicts the heat capacity increase upon unfolding as $\Delta C_p^0 = 6.34$ kcal/molK for the pretransition and $\Delta C_p^0 = 17.19$ kcal/molK for the main transition, consistent with the number of amino acids involved. The DSC-measured temperature profile of the free energy

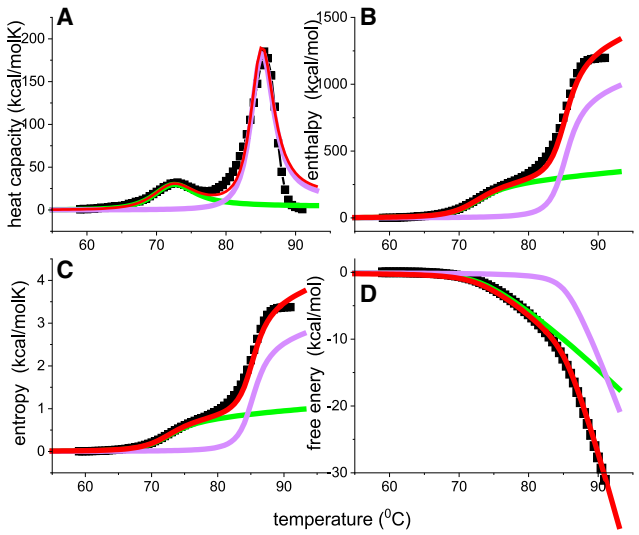

FIGURE 3 Thermal unfolding of monoclonal antibody mAb at pH 6.2. (■) DSC experiment. Solid lines are simulations with the Zimm-Bragg theory: green, pretransition; violet, main transition; red, sum of pre- and main transition. (*A*) Molar heat capacity. (*B*) Unfolding enthalpy. (*C*) Unfolding entropy. (*D*) Free energy. Simulation parameters: $h_0 = 1.1$ kcal/mol, $c_v = 7.0$ cal/molK. Pretransition: $T_0 = 73°C$, $\nu_{pre} = 263$, $\sigma = 5 \times 10^{-5}$. Main transition: $T_0 = 85.4°C$, $\nu_{main} = 880$, $\sigma = 2 \times 10^{-5}$. Data taken from reference (13).

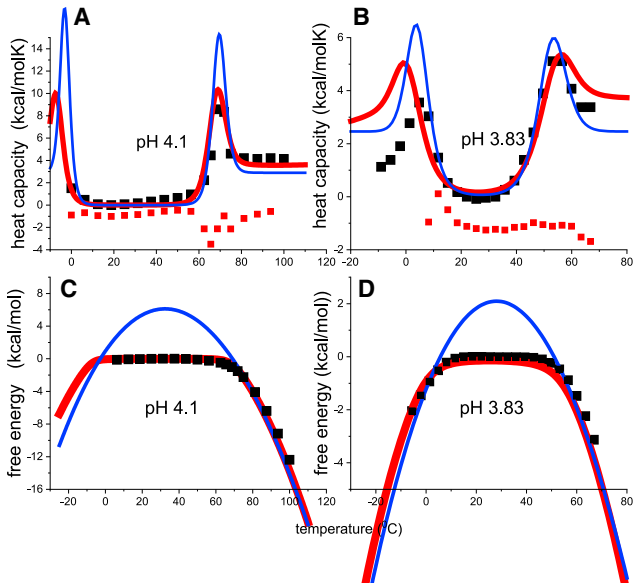

FIGURE 4 Unfolding of metmyoglobin at acidic pH. (■) Experimental data taken from reference (16). Red lines: simulations with the multistate cooperative Zimm-Bragg theory (fit parameters listed in Table 1). (red ■) Differences between DSC data and the Zimm-Bragg simulation (shifted in *B* by −1 kcal/molK for better visibility). Blue lines: two-state model. (*A*) $C_p(T)$ at pH 4.1 (Fig. 13 in reference (16)). (*B*) $C_p(T)$ at pH 3.83 (Fig. 12 in reference (16)). (*C* and *D*) Free energies calculated using the heat capacity data shown in (*A*) and (*B*).

follows the same pattern as observed for lysozyme and gpW62. The free energy of the native mAb is zero up to about 65°C followed by a biphasic decrease. As shown in Fig. 3 *D*, the contributions of the pretransition (*green*) and the main transition (*violet*) are well separated. The multistate partition function Z(T) precisely predicts this biphasic behavior. The free energy per residue is $g_{cal} = -30 \pm 1$ cal/mol for both pre- and main transition and thus clearly smaller than those of lysozyme (−47 cal/mol) and gpW62 (−136 cal/mol). Neither the pretransition nor the main transition can be simulated with the two-state model.

Heat and cold denaturation of metmyoglobin

A protein that is stable at ambient temperature can be unfolded by heating or, less commonly, by cooling. Cold denaturation of most proteins occurs at subzero temperatures. Rather drastic conditions are needed to shift cold denaturation above 0°C (e.g., addition of denaturants, low or high pH). DSC experiments reporting cold denaturation or at least partial cold denaturation are available for metmyoglobin (16), staphylococcus nuclease (42), β-lactoglobulin (43), streptomyces subtilisin inhibitor (44), or thioredoxin (45).

Metmyoglobin (153 residues) consists of 8 α-helical regions connected by loops (46). DSC at pH 4.1 (Fig. 4 *A*) displays heat denaturation at $T_0 = 69°C$ and cold denaturation starting at 3°C (data from Fig. 13 of reference (16)). Heat denaturation of the already partially destabilized protein is characterized by $\Delta H_{cal} = 146$ kcal/mol, $\Delta S_{cal} = 0.431$ kcal/mol, and $\Delta G_{cal} = -6.4$ kcal/mol. The ratio $\Delta H_{cal}/\Delta S_{cal} = 339$ K = 66°C is consistent with the $C_p(T)$ maximum. The unfolding entropy per residue is $s_{cal} = 2.81$cal/molK. Quasielastic neutron scattering (QENS) yields $s_{QENS} = 10$ J/molK = 2.39 cal/molK for the unfolding of myoglobin with 66% α-helix content (Fig. 10 in reference (47), Fig. 9 in reference (48)).Extrapolation to 100% α-helix results in $s_{QENS} = 3.63$ cal/molK. Inspection of Fig. 4 *A* shows that the Zimm-Bragg theory (fit parameters in Table 1) provides a clearly better fit of $C_p(T)$ than the two-state model (fit parameters $\Delta H_0 = 112$ kcal/mol, $\Delta C_p^0 = 2.9$ kcal/molK).

At pH 3.83, metmyoglobin is even more destabilized. DSC reports two unfolding transitions with $C_p(T)$ maxima at $T_{cold} = 8°C$ and $T_0 = 56.5°C$ (Fig. 4 *B*). The thermodynamic properties of heat unfolding are $\Delta H_{cal} = 96$ kcal/mol, $\Delta S_{cal} = 0.291$, and $\Delta H_{cal}/\Delta S_{cal} = 329.9$ K = 56.9°C. Cold denaturation is not the mirror image of heat denaturation as unfolding enthalpy and entropy are much smaller with $\Delta H_{cold} \sim 53.8$ kcal/mol and $\Delta S_{cold} \sim 0.193$ kcal/molK, respectively. $\Delta H_{cold}/\Delta S_{cold} = 274$ K = 1°C is lower than the experimental $T_{cold} = 8°C$. The free energy profile is displayed in Fig. 4 *D*. DSC yields a zero free energy for the native

TABLE 1 Thermal unfolding. Differential scanning calorimetry (DSC) and parameters of the Zimm-Bragg theory.

		DSC	DSC	DSC	DSC	DSC	ZB	Zimm-Bragg theory	ZB	ZB
		ΔH_{cal}	$h_{cal} = \Delta H_{cal}/\nu$	$s_{cal} = \Delta S_{cal}/\nu$	$g_{cal} = \Delta G_{cal}/\nu$	ΔC_p^{0}[i]	H_{con}[k]	h_0	c_ν	
Protein	N	kcal/mol	kcal/mol	cal/molK	kcal/mol	kcal/molK	kcal/mol	kcal/mol	cal/molK	σ
Native protein → unfolded protein										
gpW62[a]	62	91.7	1.48	4.34	−0.131	0.9	66.2	1.26	5	5×10^{-4}
Ubiquitin[b]	74	89.7	1.21	3.41	−0.067	1.04	68.1	1.06	4.3	1×10^{-6}
Lysozyme[c]	129	147.2	1.14	3.39	−0.047	2.28	113.3	0.99	6	1×10^{-6}
Metmyoglobin[d]	153	178.1	1.16	3.32	−0.039	2.89	142	1.08	7	7×10^{-6}
mAb pre[e]	263	290.6	1.10	3.11	−0.031	4.7	244	1.1	7	5×10^{-5}
mAb main[e]	880	1020	1.16	3.23	−0.033	17	900	1.1	7	2×10^{-5}
Destabilized protein → unfolded protein										
Metmyoglobin pH 12[f]	145	144.7	1.00	3.04	−0.048	2.54	93.7	0.75	7	1×10^{-5}
Metmyoglobin pH 4.1[g]	145	141.0	0.97	2.90	−0.044	3.58	70.5	0.6	10	2×10^{-6}
Metmyoglobin pH 3.84[h]	100	96.0	0.96	2.91	−0.031	3.74	43.8	0.6	15	7×10^{-5}
			average = 1.13					average = 0.95		
			SD = 0.16					SD = 0.3		

[a]Reference (15), Fig. 4 *A* (this work: Figs. 2 and 5 *A*).
[b]Reference (17), Fig. 1 (this work: Fig. 5 *B*).
[c]Reference (10), Fig. 8 (this work: Figs. 1 and 5 *C*).
[d]Reference (16), Fig. 3 *B*, pH 10.7 (this work: Fig. 5 *D*).
[e]Reference (13) (this work: Fig. 3).
[f]Reference (16), Fig. 3 *B* (no simulation shown).
[g]Reference (16) Fig. 13 (this work: Fig. 4 *A* and *C*).
[h]Reference (16) Fig. 12 (this work: Fig. 4 *B* and *D*).
[i]DSC-measured increase in molar heat capacity upon protein unfolding.
[k]Conformational unfolding enthalpy proper, calculated with the Zimm-Bragg theory by setting $c_\nu = 0$.

protein and negative free energies for heat and cold denaturation. This trapezoidal temperature profile is correctly predicted by the Zimm-Bragg theory. The specifics in the simulation of cold denaturation are a large heat capacity c_ν and a small unfolding enthalpy h_0 (cf. Table 1). The two-state model predicts a parabolic profile and assigns a large positive free energy to the native protein.

Metmyoglobin at pH 3.83 was analyzed previously by a hierarchical algorithm defining a partition function in terms of multiple levels of interacting folding units (49). The model reproduces an idealized, symmetrical shape of the heat capacity $C_p(T)$ and a parabolic free energy function.

Table 1 summarizes the DSC results and the Zimm-Bragg fit parameters of all proteins discussed. The table includes additional measurements of metmyoglobin at pH 10 and 12 and of ubiquitin (17), for which no simulations are shown.

DISCUSSION

Proteins in solution do not show a simple, two-state equilibrium between a fully folded and a fully unfolded conformation. Depending on temperature, they form a complex mixture of many short-lived intermediates. Here, we present a new model, which predicts the important thermodynamic functions, enthalpy, entropy, and free energy, on the basis of molecular parameters only. The performance of the model is demonstrated by comparison with DSC experiments. The Zimm-Bragg theory provides excellent simulations of the temperature course of all thermodynamic functions reported by DSC. With this model we obtain insights into the cooperativity and dynamics of protein folding.

Protein stability

The most relevant parameter of protein stability is the midpoint temperature of unfolding T_0. Protein unfolding can be approximated by a first-order phase transition, and T_0 is determined by $T_0 = \Delta H_{cal}/\Delta S_{cal}$. ΔH_{cal} and ΔS_{cal} are the DSC-measured unfolding enthalpy and entropy, respectively. Minor changes in ΔH_{cal} or ΔS_{cal} produce distinctive shifts in T_0. The ultrafast folder gpW62 (62 aa) and ubiquitin (74 aa) are short proteins with almost identical unfolding enthalpies of 91.7 and 89.7 kcal/mol, respectively. Nevertheless, their transition temperatures are ∼20°C apart with gpW62 at 67°C and ubiquitin at 89.5°C. The difference is caused by the larger gpW62 entropy ΔS_{cal} = 0.269 kcal/molK compared with ΔS_{cal} = 0.25 kcal/molK of ubiquitin. The difference becomes even more

obvious on a per residue basis with $s_{cal} = \Delta S_{cal}/\nu = 4.34$ kcal/mol for gpW62 and $s_{cal} = 3.41$ kcal/mol for ubiquitin. Likewise, very small differences in enthalpy and entropy cause the 12°C difference in the midpoint temperatures of the two mAb domains. A priori predictions of T_0 therefore require highly precise molecular dynamics (MD) calculations of unfolding enthalpy and entropy.

In a true first-order phase transition (e.g., melting of ice) the heat ΔH_{cal} is absorbed at the constant temperature T_0 and the heat capacity is a sharp peak (singularity). In contrast, ΔH_{cal} in protein unfolding is absorbed over 20–60°C and the heat capacity $C_p(T)$ is a broad peak. In particular, and not generally recognized, the relation $\Delta H_{cal} = T_0 \Delta S_{cal}$ is limited to the overall reaction, but not applicable to the measured heat $H(T_0)$ and entropy $S(T_0)$. Considering lysozyme as an example, the DSC-measured heat absorbed up to T_0 is $H(T_0) = 63.4$ kcal/mol (Eq. 10) and is less than half of the total heat of 147.2 kcal/mol). The corresponding entropy is $S(T_0) = 0.191$ kcal/molK (Eq. 11). As $H(T_0) < T_0 S(T_0)$ this results in a negative free energy $G(T_0) = -0.677$ kcal/mol (Eq. 12), more realistic for a ~50% unfolded protein than the zero free energy predicted by the two-state model. Analogous results are obtained for all proteins discussed here.

The two hallmarks of the two-state model, that is, the positive free energy of the native protein and the zero free energy of the 1:1 folded/unfolded mixture, are thus not confirmed by DSC. Instead, the free energy shows a trapezoidal shape that is precisely predicted by the new Zimm-Bragg folding model.

Molecular unfolding enthalpy h(T)

The Zimm-Bragg parameter h_0 is an average value of all types of interactions, independent of specific conformations (α-helix, β-sheet, ionic interactions, etc.). h_0 is close to the calorimetric average $h_{cal} = \Delta H_{cal}/\nu$. Metmyoglobin is an α-helical protein and the average enthalpy of the native protein (pH 10) is $h_{cal} = 178/153 = 1.16$ kcal/mol (Fig. 3 in reference (16)) while $h_0 = 1.08$ kcal/mol in the Zimm-Bragg simulation. For the ~50% α-helical apolipoprotein A1 the DSC result is $h_{cal} = 1.08 \pm 0.07$ kcal/mol and the Zimm-Bragg parameter $h_0 = 1.1$ kcal/mol (9). Lysozyme, a globular protein with mainly β-sheet structure, yields $h_{cal} = 1.14$ kcal/mol and $h_0 = 0.99$ kcal/mol (pH 2.5) (10). A comparison of a larger set of proteins has led to the conclusion that the Zimm-Bragg parameter is $h_0 = 1.1 \pm 0.2$ kcal/mol (10).

The enthalpy h_0 is usually associated with the opening of an α-helix hydrogen bond (26,30–32). However, MD calculations have led to the conclusion that "hydrogen bond formation contributes little to helix stability [...] The major driving force for helix is associated with interactions, including van der Waals interactions, in the close packed helix conformation and the hydrophobic effect" (50). This is supported by experimental results obtained with short alanine-based peptides, where hydrophobic interactions play the dominant role in stabilizing isolated α-helices (33).

Cold denaturation

Cold denaturation has been proposed as a tool to measure protein stability (51). The heat capacity c_v is a new parameter in the Zimm-Bragg theory leading to a second unfolding transition at low temperature. The temperature difference between heat and cold denaturation is given by $\Delta T = h_0/c_v$ (Eq. 5). Cold denaturation near ambient temperature thus requires a small h_0 and a large c_v. This is confirmed by metmyoglobin at pH 3.83, where h_0 is distinctly reduced to $h_0 = \sim 0.6$ kcal/mol and c_v is increased to $c_v = 10–15$ cal/molK. In general, proteins with $h_0/c_v \geq 100$ K display cold denaturation at very low subzero temperatures.

Molecular unfolding entropy

MD calculations consider all possible degrees of dihedral freedom of each amino acid residue in sampling the conformational space. In contrast, the Zimm-Bragg theory is an algorithm that differentiates only between folded and nonfolded amino acid residues, independent of the specific conformation. However, the theory makes predictions, solidly based on experimental data, that can be compared with MD calculations. The temperature course of the entropy is a good example. The entropy S(T) can be calculated with the Zimm-Bragg theory according to Eq. 8. The excellent agreement with the experimental data is displayed in Figs. 1, 2, and 3. In Fig. 5 we have repeated these calculations, including also ubiquitin, for the much larger temperature range of 298–498 K as this is the temperature interval of the "Dynameomics Entropy Dictionary" (18).

By averaging some 800 MD calculations the Dynameomics Entropy Dictionary provides the unfolding entropies of all amino acids when heated from the native state (298 K) to the fully denatured state (498 K). Using Table 2 in reference (18), we calculated the MD unfolding entropies at 498 K for the specific amino acid sequences of, gpW62 (62 aa), ubiquitin (74 aa), lysozyme (129 aa), and metmyoglobin (153 aa). The results are shown in Fig. 5 by the magenta data points at 498 K. The error bars were also calculated for each amino acid sequence using reference (18). In parallel, the Zimm-Bragg simulations were extended to 498 K, with the same parameters as deduced from $C_p(T)$ at low temperature. This extrapolation is in excellent

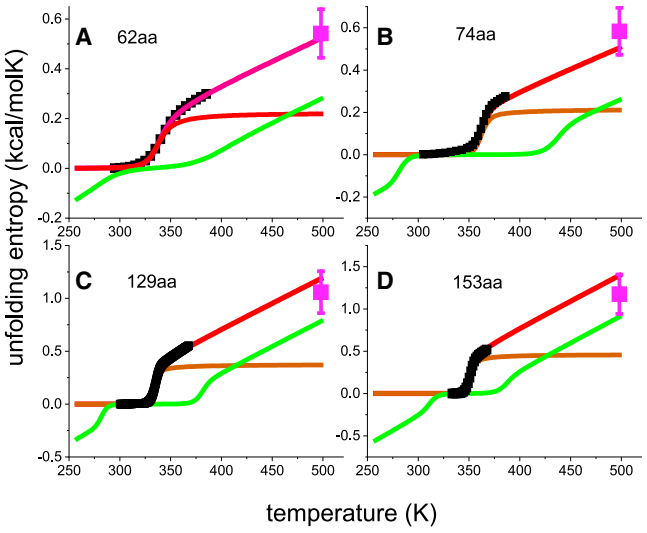

FIGURE 5 Unfolding entropy. (■) Experimental data. (magenta ■) Dynameonics Entropy Dictionary (18). (*A*) gpW62 (15). (*B*) Ubiquitin (17) (Fig. 1 in reference (17)). (*C*) Lysozyme (10) (*D*) Metmyoglobin (16) (Fig. 3 in reference (16), pH 10). Red lines: Zimm-Bragg total entropy. Brown lines: conformational entropy proper. Green lines: contribution of the heat capacity c_v.

agreement with the Dynameomics Entropy Dictionary and supports the relevance of the molecular parameters of the Zimm-Bragg theory in protein unfolding.

The entropy S(T) (red) can be divided into the conformational entropy proper (brown line, $h_0 = \text{const.}$, $c_v = 0$) and the contribution of the heat capacity term c_v (green line, $h_0 = 0$, $c_v = \text{const.}$). The h_0 term determines S(T) up to the end of the conformational transition, where $\Theta_U \sim 0.85–0.9$. However, it takes another temperature increase of more than 100°C to reach complete denaturation.

The average entropy is $s_{cal} = \Delta S_{cal}/\nu = 3.25 \pm 0.25$ cal/molK per residue (Table 1) and involves at least three single bonds. The entropy per single bond is ~1.1 cal/molK and can be compared with other phase transitions. The solid-fluid transition of long-chain paraffins yields a much larger entropy of 1.8–2.7 cal/molK per C-C bond. The gel-to-liquid crystal transition of phospholipid bilayers leads 1.25–1.6 cal/molK per C-C bond (Table 2.7, p. 47 in reference (52)). As judged by the small entropy of 1.1 cal/molK, the unfolded proteins are still characterized by a restricted motion of their molecular constituents. For metmyoglobin it was noted that "the unfolded state retains some residual ellipticity, which may be caused by the fluctuating α-helical conformation of the unfolded polypeptide chain" (16). This conclusion is supported by neutron spin-echo spectroscopy studies on apomyoglobin where secondary structural elements and α-helices are found to be transiently formed at denaturation or molten globule conditions (53). Likewise, the combination of FRET, NMR, and SAX techniques has revealed a residual structure in denatured ubiquitin (54).

Protein cooperativity

The folding/unfolding transition of proteins is a cooperative process. The Zimm-Bragg theory provides a quantitated measure of cooperativity. In fact, the cooperativity parameter σ plays an important role in the energy and kinetics of the folding process as it determines the free energy to start a new fold within an unfolded region (nucleation) (55). The corresponding free energy is

$$\Delta G_\sigma = -RT_0 \ln(\sigma). \tag{14}$$

A large σ corresponds to low cooperativity and to a small nucleation energy ΔG_σ. gpW62 has a cooperativity parameter $\sigma = 5 \times 10^{-4}$ and hence a nucleation energy of $\Delta G_\sigma = 5.13$ kcal/mol. In contrast, lysozyme unfolding is highly cooperative with $\sigma = 1 \times 10^{-6}$ and $\Delta G_\sigma = 9.21$ kcal/mol. The low gpW62 nucleation energy makes gpW62 folding easier than that of lysozyme. If ΔG_σ is assumed to be correlated with the kinetic activation energy, then gpW62 folding should be ~500 times faster than that of lysozyme. In infrared T-jump experiments of gpW62, the return to equilibrium followed a single exponential with a relaxation time of $\tau = 15.7$ μs at 57°C (15). In contrast, lysozyme was found to fold in a two-step mechanism with a slow nucleation ($\tau = 14$ ms) followed by a fast growth step ($\tau = 300$ μs) at room temperature (56).

Free energy of unfolding

The free energy of unfolding ΔG_{cal} scales with the size of the protein, and a per residue free energy $g_{cal} = \Delta G_{cal}/\nu$ is better suited for comparative purposes. According to the Zimm-Bragg theory g_{cal} can be approximated by

$$g_{cal} \simeq h(T_{end})(1 - T_{end}/T_0) = -(h_0 + c_v \Delta T)(\Delta T/T_0). \tag{15}$$

T_{end} denotes the temperature at the end of the conformational transition and $\Delta T = T_{end} - T_0$ is the halfwidth of the transition. The approximation Eq. 15 agrees within 2% with the DSC measurement for the proteins listed in Table 1. The free energy per amino acid residue varies between $g_{cal} = -131$ cal/mol for gpW62 to $g_{cal} = -33$ cal/mol for mAb. In parallel, the width of the transition decreases from 65°C for gpW62 to 20°C for mAb (large domain). An approximately linear relationship between g_{cal} and ΔT is predicted by Eq. 15 and is confirmed by DSC, that is, a large g_{cal} correlates with a broad transition.

Considering the three parameters T_0, g_{cal}, and ΔT, gpW62 is the least stable protein discussed here.

CONCLUSIONS

The protein folding/unfolding transition is a highly cooperative process which cannot be adequately simulated by the noncooperative two-state model. A multistate cooperative model is provided by the Zimm-Bragg theory. Here, we combined the partition function of the Zimm-Bragg theory with statistical-mechanical thermodynamics. The model predicts the DSC-measured enthalpy, entropy, and free energy of protein unfolding with molecular parameters, which have well-defined physical meanings. We analyzed the DSC thermograms of proteins of different chain length and structure. We show that the temperature profile of the free energy is characterized by a trapezoidal shape. The new model is in excellent agreement with this experimental finding. The present model reveals whether a protein is a fast or a slow folder and predicts heat as well as cold denaturation. The results of the new model can be compared with MD calculations. Using the molecular parameters derived from DSC at relatively low temperature the entropy at complete unfolding at 498 K was calculated for four different proteins. The results are in excellent agreement with the predictions of the Dynameomics Entropy Dictionary and quasi elastic neutron scattering.

AUTHOR CONTRIBUTIONS

J.S. developed the theory. J.S. and A.S. wrote the manuscript.

DECLARATION OF INTERESTS

The authors declare no competing interests.

ACKNOWLEDGMENTS

Stiftung zur Förderung der biologischen Forschung, Basel, Switzerland.

REFERENCES

1. Murphy, K. P., and E. Freire. 1992. Thermodynamics of structural stability and cooperative folding behavior in proteins. *Adv. Protein Chem.* 43:313–361. https://doi.org/10.1016/s0065-3233(08)60556-2. https://www.ncbi.nlm.nih.gov/pubmed/1442323.
2. Privalov, P. L., and S. J. Gill. 1988. Stability of protein-structure and hydrophobic interaction. *Adv. Protein Chem.* 39:191–234.
3. Privalov, P. L. 1990. Cold denaturation of proteins. *Crit. Rev. Biochem. Mol.* 25:281–305. https://doi.org/10.3109/10409239009090612.
4. Ibarra-Molero, B., and J. M. Sanchez-Ruiz. 2008. Statistical differential scanning calorimetry: probing protein folding-unfolding ensembles. *RSC Biomol. Sci.* 85–105. https://doi.org/10.1039/9781847558282-00085.
5. Brandts, J. F. 1964. Thermodynamics of protein denaturation. I. Denaturation of chymotrypsinogen. *J. Am. Chem. Soc.* 86:4291. https://doi.org/10.1021/ja01074a013.
6. Doig, A. J. 2002. Recent advances in helix-coil theory. *Biophys. Chem.* 101-102:281–293. http://www.ncbi.nlm.nih.gov/pubmed/12488008.
7. Wieprecht, T., O. Apostolov, …, J. Seelig. 1999. Thermodynamics of the alpha-helix-coil transition of amphipathic peptides in a membrane environment: implications for the peptide-membrane binding equilibrium. *J. Mol. Biol.* 294:785–794. https://doi.org/10.1006/jmbi.1999.3268. http://www.ncbi.nlm.nih.gov/pubmed/10610796.
8. Zehender, F., A. Ziegler, …, J. Seelig. 2012. Thermodynamics of protein self-association and unfolding. The case of apolipoprotein A-I. *Biochemistry.* 51:1269–1280. https://doi.org/10.1021/Bi2013799.
9. Schulthess, T., H. J. Schonfeld, and J. Seelig. 2015. Thermal unfolding of apolipoprotein A-1. Evaluation of methods and models. *Biochemistry.* 54:3063–3075. https://doi.org/10.1021/acs.biochem.5b00238. http://www.ncbi.nlm.nih.gov/pubmed/25907854.
10. Seelig, J., and H.-J. Schönfeld. 2016. Thermal protein unfolding by differential scanning calorimetry and circular dichroism spectroscopy two-state model versus sequential unfolding. *Q. Rev. Biophys.* 49:e9. https://doi.org/10.1017/S0033583516000044.
11. Eckhardt, D., X. Li-Blatter, …, J. Seelig. 2018. Cooperative unfolding of apolipoprotein A-1 induced by chemical denaturation. *Biophys. Chem.* 240:42–49. https://doi.org/10.1016/j.bpc.2018.05.005. https://www.ncbi.nlm.nih.gov/pubmed/29885564.
12. Seelig, J. 2018. Cooperative protein unfolding. A statistical-mechanical model for the action of denaturants. *Biophys. Chem.* 233:19–25. https://doi.org/10.1016/j.bpc.2017.12.001. https://www.ncbi.nlm.nih.gov/pubmed/29232602.
13. Garidel, P., A. Eiperle, …, J. Seelig. 2020. Thermal and chemical unfolding of a monoclonal IgG1 antibody: application of the multistate Zimm-Bragg theory. *Biophys. J.* 118:1067–1075. https://doi.org/10.1016/j.bpj.2019.12.037. https://www.ncbi.nlm.nih.gov/pubmed/32049058.
14. Li-Blatter, X., and J. Seelig. 2019. Thermal and chemical unfolding of lysozyme. Multistate Zimm-Bragg theory versus two-state model. *J. Phys. Chem. B.* 123:10181–10191. https://doi.org/10.1021/acs.jpcb.9b08816. https://www.ncbi.nlm.nih.gov/pubmed/31686511.
15. Fung, A., P. Li, …, V. Munoz. 2008. Expanding the realm of ultrafast protein folding: gpW, a midsize natural single-domain with alpha+beta topology that folds downhill. *J. Am. Chem. Soc.* 130:7489–7495. https://doi.org/10.1021/ja801401a. https://www.ncbi.nlm.nih.gov/pubmed/18479088.
16. Privalov, P. L., Y. V. Griko, …, V. P. Kutyshenko. 1986. Cold denaturation of myoglobin. *J. Mol. Biol.* 190:487–498. https://doi.org/10.1016/0022-2836(86)90017-3.
17. Ibarra-Molero, B., G. I. Makhatadze, and J. M. Sanchez-Ruiz. 1999. Cold denaturation of ubiquitin. *Biochim. Biophys. Acta.* 1429:384–390. http://www.ncbi.nlm.nih.gov/pubmed/9989223.
18. Towse, C. L., M. Akke, and V. Daggett. 2017. The dynameomics entropy dictionary: a large-scale assessment of conformational entropy across protein fold space. *J. Phys. Chem. B.* 121:3933–3945. https://doi.org/10.1021/acs.jpcb.7b00577.
19. Pfeil, W., and P. L. Privalov. 1976. Thermodynamic investigations of proteins. II. Calorimetric study of lysozyme denaturation by guanidine hydrochloride. *Biophys. Chem.* 4:33–40. https://www.ncbi.nlm.nih.gov/pubmed/1247649.
20. Privalov, G., V. Kavina, …, P. L. Privalov. 1995. Precise scanning calorimeter for studying thermal-properties of biological macromolecules in dilute-solution. *Anal. Biochem.* 232:79–85. https://doi.org/10.1006/abio.1995.9957.
21. Durowoju, I. B., K. S. Bhandal, …, M. Kirkitadze. 2017. Differential scanning calorimetry—a method for assessing the thermal

stability and conformation of protein antigen. *J. Vis. Exp.* 121:e55262. https://doi.org/10.3791/55262.

22. Privalov, P. L. 1997. Thermodynamics of protein folding. *J. Chem. Thermodyn.* 29:447–474. https://doi.org/10.1006/jcht.1996.0178.
23. Privalov, P. L., and A. I. Dragan. 2007. Microcalorimetry of biological macromolecules. *Biophys. Chem.* 126:16–24. https://doi.org/10.1016/j.bpc.2006.05.004. http://www.ncbi.nlm.nih.gov/pubmed/16781052.
24. Seelig, J. 2022. Free energy in thermal and chemical protein unfolding. *In* Gibbs Energy and Helmholtz Energy: Liquids, Solutions and Vapours. E. Wilhelm and T. M. Letcher, eds. Royal Society of Chemistry, pp. 363–378.
25. Zimm, B. H., and J. K. Bragg. 1959. Theory of the phase transition between helix and random coil in polypeptide chains. *J. Chem. Phys.* 31:526–535. https://doi.org/10.1063/1.1730390.
26. Zimm, B. H., P. Doty, and K. Iso. 1959. Determination of the parameters for helix formation in poly-gamma-benzyl-L-glutamate. *Proc. Natl. Acad. Sci. U S A.* 45:1601–1607. http://www.ncbi.nlm.nih.gov/pubmed/16590552.
27. Davidson, N. 1962. *In* Statistical Mechanics. Mac Graw-Hill, p. 385.
28. Sirotkin, V. A., and R. Winter. 2010. Volume changes associated with guanidine hydrochloride, temperature, and ethanol induced unfolding of lysozyme. *J. Phys. Chem. B.* 114:16881–16886. https://doi.org/10.1021/jp105627w.
29. Chen, C. R., and G. I. Makhatadze. 2017. Molecular determinant of the effects of hydrostatic pressure on protein folding stability. *Nat. Commun.* 8:14561.
30. Rialdi, G., and J. Hermans. 1966. Calorimetric heat of helix-coil transition of poly-L-glutamic acid. *J. Am. Chem. Soc.* 88:5719. https://doi.org/10.1021/Ja00976a007.
31. Chou, P. Y., and H. A. Scheraga. 1971. Calorimetric measurement of enthalpy change in isothermal helix-coil transition of poly-L-lysine in aqueous solution. *Biopolymers.* 10:657. https://doi.org/10.1002/bip.360100406.
32. Luo, P., and R. L. Baldwin. 1997. Mechanism of helix induction by trifluoroethanol: a framework for extrapolating the helix-forming properties of peptides from trifluoroethanol/water mixtures back to water. *Biochemistry.* 36:8413–8421. https://doi.org/10.1021/bi9707133. http://www.ncbi.nlm.nih.gov/pubmed/9204889.
33. Marqusee, S., V. H. Robbins, and R. L. Baldwin. 1989. Unusually stable helix formation in short alanine-based peptides. *Proc. Natl. Acad. Sci. U S A.* 86:5286–5290. http://www.ncbi.nlm.nih.gov/pubmed/2748584.
34. Eisenberg, D., and D. Crothers. 1979. Calculation of the energy using the system partition function. *In* Physical Chemistry with Applications to the Life Sciences. B. Rhame and M. Moore, eds. The Benjamin/Cummings Publishing Company, Inc., p. 675.
35. Baumann, R. P. 1992. Evaluation of thermodynamic properties. *In* Modern Thermodynamics with Statistical Mechanics. R. A. McConnin, ed. Macmillan Publishing Company, p. 341.
36. Privalov, P. L., and G. I. Makhatadze. 1990. Heat capacity of proteins. II. Partial molar heat capacity of the unfolded polypeptide chain of proteins: protein unfolding effects. *J. Mol. Biol.* 213:385–391. https://doi.org/10.1016/S0022-2836(05)80198-6. http://www.ncbi.nlm.nih.gov/pubmed/2160545.
37. Myers, J. K., C. N. Pace, and J. M. Scholtz. 1995. Denaturant m values and heat capacity changes: relation to changes in accessible surface areas of protein unfolding. *Protein Sci.* 4:2138–2148. https://doi.org/10.1002/pro.5560041020. http://www.ncbi.nlm.nih.gov/pubmed/8535251.
38. Meixner, J. 1943. On the thermodynamics of the irreversible processes in gasses with chemically reacting, dissociating and stimulable components. *Ann. Phys. (Berlin).* 43:244–270.
39. Prigogine, I., P. Outer, and C. Herbo. 1948. Affinity and reaction rate close to equilibrium. *J. Phys. Colloid Chem.* 52:321–331. https://doi.org/10.1021/j150458a004.
40. Prigogine, I. 1967. *In* Thermodynamics of Irreversble Processes. Interscience Publisher, pp. 23–56.
41. Garidel, P., W. Kliche, …, M. Thierolf. 2010. Characterisation of proteins and related analytical techniques, HC. *In* Protein Pharmaceuticals: Formulation, Analytics and Delivery. Editio-Cantor Verlag, pp. 44–89.
42. Griko, Y. V., P. L. Privalov, …, S. Y. Venyaminov. 1988. Cold denaturation of staphylococcal nuclease. *Proc. Natl. Acad. Sci. U S A.* 85:3343–3347. https://doi.org/10.1073/pnas.85.10.3343.
43. Griko, Y. V., and P. L. Privalov. 1992. Calorimetric study of the heat and cold denaturation of beta-lactoglobulin. *Biochemistry.* 31:8810–8815. https://doi.org/10.1021/bi00152a017. https://www.ncbi.nlm.nih.gov/pubmed/1390668.
44. Tamura, A., K. Kimura, …, K. Akasaka. 1991. Cold denaturation and heat denaturation of streptomyces subtilisin inhibitor. 1. CD and DSC studies. *Biochemistry.* 30:11307–11313. https://doi.org/10.1021/bi00111a017.
45. Romero-Romero, M. L., A. Ingles-Prieto, …, J. M. Sanchez-Ruiz. 2011. Highly anomalous energetics of protein cold denaturation linked to folding-unfolding kinetics. *PLoS One.* 6:e23050. https://doi.org/10.1371/journal.pone.0023050.
46. Urayama, P., G. N. Phillips, Jr., and S. M. Gruner. 2002. Probing substates in sperm whale myoglobin using high-pressure crystallography. *Structure.* 10:51–60. https://doi.org/10.1016/s0969-2126(01)00699-2. https://www.ncbi.nlm.nih.gov/pubmed/11796110.
47. Stadler, A. M., M. M. Koza, and J. Fitter. 2015. Determination of conformational entropy of fully and partially folded conformations of holo- and apomyoglobin. *J. Phys. Chem. B.* 119:72–82. https://doi.org/10.1021/jp509732q.
48. Stadler, A. M., F. Demmel, …, T. Seydel. 2016. Picosecond to nanosecond dynamics provide a source of conformational entropy for protein folding. *Phys. Chem. Chem. Phys.* 18:21527–21538. https://doi.org/10.1039/c6cp04146a.
49. Freire, E., and K. P. Murphy. 1991. Molecular-basis of cooperativity in protein folding. *J. Mol. Biol.* 222:687–698. https://doi.org/10.1016/0022-2836(91)90505-Z.
50. Yang, A. S., and B. Honig. 1995. Free energy determinants of secondary structure formation: I. alpha-helices. *J. Mol. Biol.* 252:351–365. https://doi.org/10.1006/jmbi.1995.0502. http://www.ncbi.nlm.nih.gov/pubmed/7563056.
51. Sanfelice, D., and P. A. Temussi. 2016. Cold denaturation as a tool to measure protein stability. *Biophys. Chem.* 208:4–8. https://doi.org/10.1016/j.bpc.2015.05.007. https://www.ncbi.nlm.nih.gov/pubmed/26026885.
52. Seelig, J. 1979. Physical properties of model membranes and biological membranes. *In* Membranes et Communication (Intercellulaire/Membranes and Intercellular Communication). R. Balian, ed. North-Holland Publishing Company, p. 1981.
53. Balacescu, L., T. E. Schrader, …, A. M. Stadler. 2020. Transition between protein-like and polymer-like dynamic behavior: internal friction in unfolded apomyoglobin depends on denaturing conditions. *Sci. Rep.* 10:1570. https://doi.org/10.1038/s41598-020-57775-4.
54. Aznauryan, M., L. Delgado, …, B. Schuler. 2016. Comprehensive structural and dynamical view of an unfolded protein from the combination of single-molecule FRET, NMR, and SAXS. *Proc. Natl. Acad. Sci. U S A.* 113:E5389–E5398. https://doi.org/10.1073/pnas.1607193113.
55. Schwarz, G., and J. Seelig. 1968. Kinetic properties and electric field effect of helix-coil transition of poly(gamma-benzyl L-glutamate) determined from dielectric relaxation measurements. *Biopolymers.* 6:1263. https://doi.org/10.1002/bip.1968.360060904.
56. Kiefhaber, T., A. Bachmann, …, C. Wagner. 1997. Direct measurement of nucleation and growth rates in lysozyme folding. *Biochemistry.* 36:5108–5112. https://doi.org/10.1021/bi9702391. https://www.ncbi.nlm.nih.gov/pubmed/9136870.